NAA-SR-7086
RADIATION EFFECTS
ON MATERIALS
39 PAGES

PRODUCTION OF VOID AND PRESSURE BY FISSION TRACK NUCLEATION OF RADIOLYTIC GAS BUBBLES DURING POWER BURSTS IN A SOLUTION REACTOR

By

P. SPIEGLER
C. F. BUMPUS, JR.
A. NORMAN

ATOMICS INTERNATIONAL

A DIVISION OF NORTH AMERICAN AVIATION, INC.
P.O. BOX 309 CANOGA PARK, CALIFORNIA

CONTRACT: AT(11-1)-GEN-8
ISSUED: DEC 30 1962

DISCLAIMER

DISTRIBUTION

This report has been distributed according to the category "Radiation Effects on Materials" as given in "Standard Distribution Lists for Unclassified Scientific and Technical Reports" TID-4500 (17th Ed.), December 15, 1961. A total of 748 copies was printed.

CONTENTS

TABLES

FIGURES

FIGURES

I. ABSTRACT AND INTRODUCTION

The Kinetic Experiment on Water Boiler (KEWB) reactor is a 50-kw aqueous homogeneous research reactor which was designed to study the safety characteristics and dynamic behavior of this class of reactors. When the reactor is placed on a short-period power transient, its aqueous uranyl sulfate fuel solution becomes rapidly supersaturated with hydrogen gas produced by the radiolysis of water. At a critical gas concentration, fission track nucleation of hydrogen bubbles occurs. The rapid formation and growth of these bubbles creates a pressure field, the so-called inertial pressure, which causes an increase in solution volume. This increase in solution volume, referred to as void, causes a loss of reactivity and constitutes an important shutdown mechanism.

This report describes the conditions under which fission track nucleation of gas bubbles occurs. It shows that the void volume and void compensated reactivity can be calculated from a knowledge of the pressure field. Simple models for the pressure field are presented which satisfactorily describe the observed pressures. The inpile capsule and KEWB experiments which confirm the validity of the mechanisms for these processes are described.

The equations and data presented in this report make it possible to predict with accuracy the onset and magnitude of the inertial pressure and the dynamic reactivity for a large class of aqueous homogeneous reactors.

II. FISSION TRACK NUCLEATION OF HYDROGEN BUBBLES IN URANYL SULFATE SOLUTIONS

During steady-state operation, or in slow transients, the gases produced by the radiolysis of water are removed continuously in the form of gas bubbles from the fuel solution. These bubbles are nucleated at various sites on the surface of the core vessel, cooling coils, and other stainless-steel surfaces in contact with the fuel. During fast transients, however, diffusion of gas from the fuel to these sites is too slow for surface nucleation to be effective. Instead, the hydrogen gas concentration increases until, at a critical concentration, the reactor behaves like a gas bubble chamber;[1] i.e., gas bubbles are nucleated by the fission tracks. Inpile capsule experiments (see Appendix A) and the KEWB experiments* have led to a rather clear picture of this nucleation process. This permits a prediction of the conditions under which fission track nucleation will occur and, hence, of the onset of inertial pressure. A detailed description of fission track nucleation is presented below.

The stability requirement for a gas bubble in a supersaturated solution is:

$$p_i = K(T)C_c = \frac{2\sigma(T)}{R_g} + p_\ell \ , \qquad \ldots(1)$$

where

p_i = internal gas pressure of bubble,

K = Henry's constant,

C_c = critical gas concentration in liquid,

σ = surface tension of liquid-gas interface,

R_g = bubble radius, and

p_ℓ = liquid pressure.

The dependence of K and σ on the temperature, T, is shown explicitly. The results for the dependence of the critical H_2 concentration on temperature are shown in Figure 1. The solid lines are calculated from Equation 1 under the assumption that the radius is fixed. The observed points were obtained from the

*For a description of the KEWB cores, refer to References 2 and 3. A summary of the various core performances can be found in Appendix B.

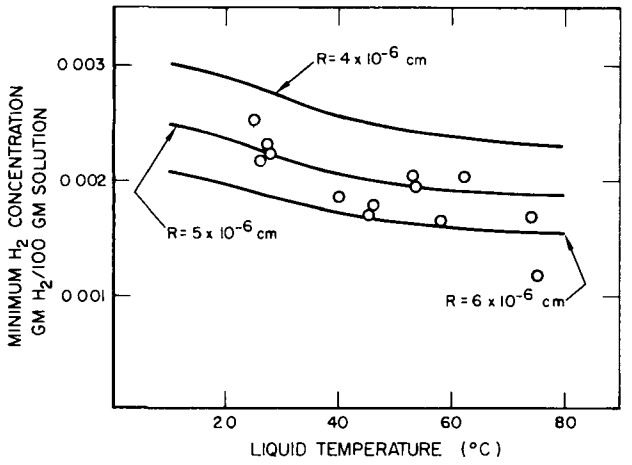

Figure 1. Critical Hydrogen Concentration as a Function of Liquid Temperature

KEWB "A" reactor and are the H_2 concentration at the center of the core when the inertial pressure makes its appearance. The fuel concentration was 180 gm U/ℓ, and the liquid pressure varied from 15 to 75-cm Hg. As can be seen, a plot of Equation 1 with a fixed radius of 5×10^{-6} cm independent of temperature gives fair agreement with the data. Figure 2 shows results for the critical hydrogen concentration as a function of liquid pressure for two values of surface tension. The solid lines are calculated from Equation 1 under the assumption that the radius is fixed at 5×10^{-6} cm. The observed points were obtained from inpile capsule experiments (see Appendix A). The circles and squares represent data obtained with σ = 75 dynes/cm and σ = 35 dynes/cm, respectively. The surface tension was reduced to 35 dynes/cm by the addition of surface active agents, either Sterox A. J. or Aerosol O. S. The fuel concentration was 250 gm U/ℓ, and the liquid temperature was 35 and 30°C for the 75 and 35 dynes/cm solutions, respectively. Here again, a plot of Equation 1 with a fixed radius of 5×10^{-6} cm adequately represents the data. Additional inpile capsule experiments at a uranium concentration of 400 gm U/ℓ were also consistent with a nucleation radius of 5×10^{-6} cm.

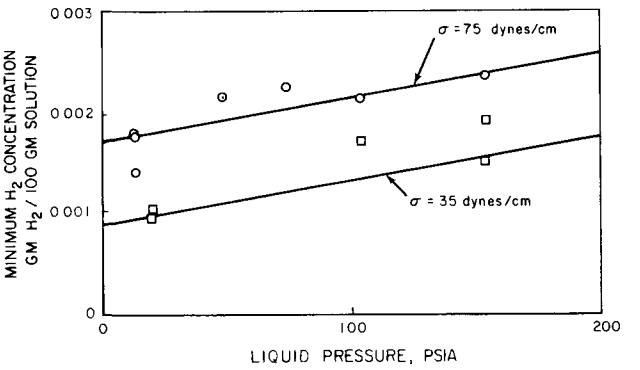

Figure 2. Critical Hydrogen Concentration as a Function of Liquid Pressure

The data thus lead to the conclusion that gas bubbles are nucleated at a fixed radius of 5×10^{-6} cm independent of temperature (20 to 80°C), liquid pressure (1 to 10 atm), surface tension (35 to 75 dynes/cm), dissolved gas concentration (1.0 to 2.5×10^{-3} gm H_2/100 gm solution) and uranium concentration (170 to 400 gm U/ℓ).

The pressure data also imply that nucleation, in agreement with Equation 1, is a threshold phenomenon; that is, the liquid pressure rises abruptly when the hydrogen gas concentration exceeds C_c. But this behavior also implies a very short lifetime for the nucleation centers formed in the fission tracks when the gas concentration is less than C_c. For example, in the 18-ℓ KEWB "B" core no pressure rise (0.1 atm is readily detectable) was observed for fission rates as high as 10^{19} fissions/sec, the gas concentration in solution being well below critical. The number of bubbles in the core is governed by

$$\frac{dN}{dt} = -\frac{N}{\ell} + S \quad , \qquad \ldots (2)$$

where

N = number of bubbles in core,

S = number of bubbles born per unit time, conservatively assumed equal to fission rate, and

ℓ = lifetime of bubble.

If S can be considered constant over time intervals much larger than ℓ, then it can be shown that a solution of Equation 2 is

$$N = S\ell \quad . \qquad \ldots (3)$$

These N bubbles should lead to an observed pressure change, Δp, given by

$$\Delta p = \frac{S\ell v_b}{K_\ell V_{core}} \qquad \ldots (4)$$

where

v_b = bubble volume,

K_ℓ = compressibility of liquid, and

V_{core} = core volume.

Using values of $\Delta p = 0.1$ atm, as a maximum value for a pressure change that might escape detection, $S = 10^{19}$ bubbles/sec, $V_{core} = 1.8 \times 10^4$ cm^3, $v_b = 5.25 \times 10^{-16}$ cm^3, and $K_\ell = 5 \times 10^{-5}$ atm^{-1}, an upper limit for ℓ of ~ 10 μsec is

obtained. Epstein and Plesset[4] have derived an analytical expression for the time of complete solution of a gas bubble in an undersaturated liquid gas solution taking surface tension effects into account. Figure 3 shows the complete solution time for a hydrogen gas bubble based on Epstein and Plesset's work. The curve for a bubble of 5×10^{-6} cm radius is in agreement with the 10 μsec lifetime provided the gas concentration is less than 50% of the critical gas concentration. The smallest observable time interval on the data recording instrumentation is 2×10^{-4} sec. Figure 3 shows that the gas concentration must be 96% of critical before the bubble lifetime reaches this value. If the bubbles were much larger, say 10^{-5} cm in radius, then, as can be seen from Figure 3, a lifetime of 2×10^{-4} sec would be achieved at a gas concentration of 87% critical, and the pressure would begin to rise smoothly before the critical concentration was achieved. If the bubbles were much smaller than 5×10^{-6} cm in radius, say 10^{-6} cm, then a lifetime of 2×10^{-4} sec would be achieved at a gas concentration of 99% critical, and the pressure rise would be even more abrupt than is observed, virtually showing a discontinuity in the initial slope of the pressure curve. In all experiments, the pressure appears rapidly, but never in the form of a discontinuity; a small curvature is always discernible at the start of pressure (see Figures 22 and 23). Thus, lifetime considerations also are consistent with a nucleation radius of 5×10^{-6} cm.

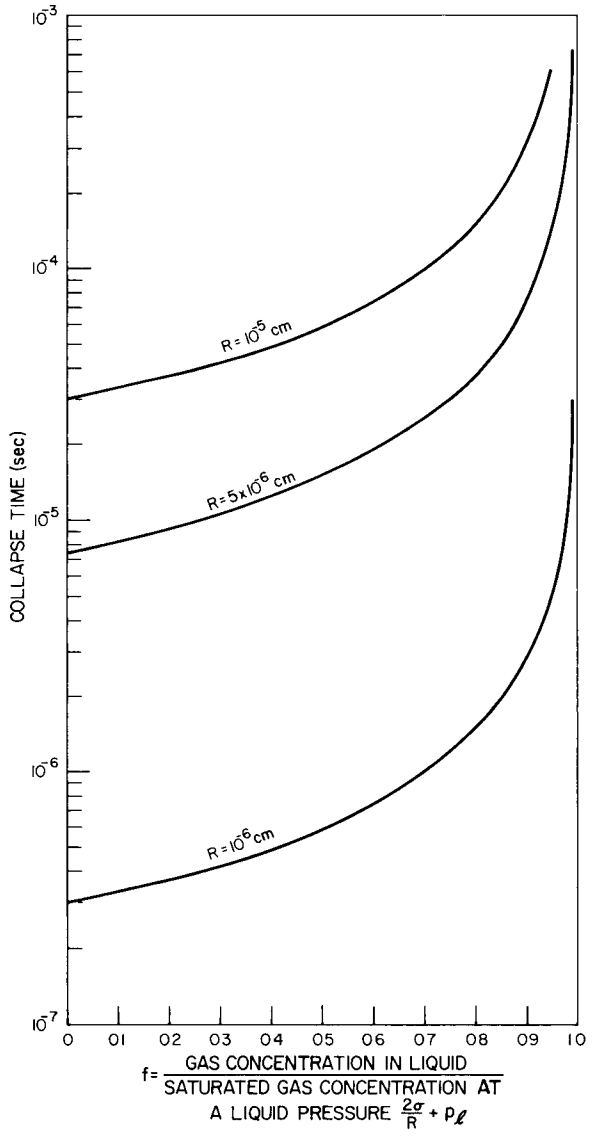

Figure 3. Collapse Time of Gas Bubble in a Uranyl Sulfate Solution as a Function of Gas Concentration

A hydrogen bubble 5 x 10^{-6} cm in radius submerged in a liquid with a surface tension of 70 dynes/cm contains 3.5 x 10^{5} H_2 molecules. For the observed G_{H_2} value of 1 molecule of H_2/100 ev, it is easily found that an energy release of 35 Mev is necessary for the production of this amount of gas.

Ghormley[5] has shown that fission tracks nucleate vapor bubbles 1.4 μ in diam in supersaturated uranyl sulfate solutions. The formation of such vapor bubbles requires an energy release of ~30 Mev and is arrived at from

$$E_b = \frac{4}{3}\pi R^3\left(p_\ell - p_v\right) + 4\pi R^2\left(\sigma - T_\ell \frac{d\sigma}{dT}\right)$$

$$+ \frac{4}{3}\pi R^3 \delta_v\left[\int_{T_\ell}^{T_v}\left(C_v\right)_v dT + L\right] + 2\pi\delta_\ell R^3\dot{R}^2 \qquad \ldots (5)$$

when

R = vapor bubble radius,

p_ℓ = liquid pressure,

p_v = vapor pressure,

σ = surface tension of liquid vapor interface,

T_ℓ = liquid temperature,

δ_v = vapor density at pressure,

δ_ℓ = liquid density,

T_v = vapor temperature,

$(C_v)_v$ = specific heat of vapor at constant volume,

L = latent heat of evaporation of liquid at temperature T_v, and

$\dot{R}$ = velocity of bubble wall.

The term $4/3\pi R^3(p_\ell - p_v)$ is the work done in creating a spherical hole of radius, R, against a liquid pressure, p_ℓ, minus the work returned by filling it with vapor at a pressure, p_v. The term $4\pi R^2\left[\sigma - (d\sigma/dT)T\right]$ represents the surface energy of the bubble. The term

$$\frac{4}{3}\pi R^3\left[\int_{T_\ell}^{T_v}(C_v)_v\,dT + L\right]$$

represents the work done in vaporizing the liquid to a temperature T_v. Finally, the term $2\pi R^3\dot{R}^2$ represents the kinetic energy imparted to the liquid. If $\dot{R}$ is well below the velocity of sound in the liquid, then the dominant term is the third.

In solutions with temperatures below boiling, an upper limit for the lifetime of a vapor bubble is given by

$$\tau = \frac{R^2}{4D} \qquad \ldots (6)$$

where D = thermal diffusivity for the liquid. Letting $R = 7 \times 10^{-5}$ cm, as observed by Ghormley, and $D = 1.5 \times 10^{-3}$ cm^2/sec, a value of $\tau = 8 \times 10^{-7}$ sec is obtained. Plesset and Zwick[6] have shown that the collapse time of small vapor bubbles differs little from the collapse of a spherical cavity as solved by Rayleigh. According to Rayleigh, such a cavity collapses in a time

$$\tau = 0.92R\left(\frac{\delta_\ell}{p_\ell}\right)^{1/2} \qquad \ldots (7)$$

Letting $R = 7 \times 10^{-5}$ cm, $\delta_\ell = 1$ gm/cc and $p_\ell = 1$ atm, a value of $\tau = 6 \times 10^{-8}$ sec is obtained. Arguments based on the pressure trace similar to those used in estimating the lifetime of gas bubbles suggest that the lifetime of a vapor bubble is not larger than 10^{-8} sec. Clearly, the lifetime computed from the pressure trace is based on the average bubble size and will be smaller than the lifetime computed from Equations 6 and 7 based on the maximum size. Moreover, Equation 7 neglects surface tension effects, which will speed the collapse of the cavity, and thus somewhat overestimates the lifetime.

The nucleation picture of gas bubbles in uranyl sulfate solutions with temperature below boiling appears, therefore, as follows: the fission fragments lose 30 Mev along the central 4 μ of the track, resulting in the formation of a mixed water vapor hydrogen bubble 1.4 μ in diam and containing $\sim 4 \times 10^5$ H_2 molecules. The vapor condenses in $\sim 10^{-8}$ sec, leaving a hydrogen bubble 5×10^{-6} cm in radius. The hydrogen bubble dissolves in about 10 μsec unless the gas concentration in solution equals or exceeds that given by Equation 1.

In applying these results toward predicting the energy release necessary for bubble nucleation in any aqueous homogeneous reactor, let the neutron flux, Φ, be specified and separable in time and space, or

$$\Phi(r, t) = \phi(r)f(t) \quad . \qquad \ldots (8)$$

The H_2 concentration at a point r and time t is then

$$C(r, t) = \int_o^t \epsilon G_{H_2} \Sigma_f \phi(r) f(t)\, dt$$

$$= \epsilon G_{H_2} \Sigma_f \phi(r) F(t) \qquad \ldots (9)$$

where

ϵ = energy release per fission,

Σ_f = fission cross section, and

G_{H_2} = number of hydrogen molecules formed per unit energy release.

When C reaches a value given by Equation 1, stable bubbles are nucleated. This will occur first in the region of peak flux. The total energy released in the core up to that moment will be

$$E_c = a_1 \Sigma_f \bar{\phi} V_{core} F(t) \qquad \ldots (10)$$

where a_1 is a constant depending on the unit system in which E is expressed, and $\bar{\phi}$ is the space average of the flux. If E is expressed in Mw-sec, then $a = 1/3 \times 10^{-16}$ Mw-sec/fission. Replacing $\phi(r)$ in Equation 9 by ϕ_p, the peak flux, and combining this with Equation 10, the following is obtained:

$$E_c = \left(\frac{V_{core}}{\epsilon G_{H_2}}\right)\frac{\bar{\phi}}{\phi_p} C_c \quad . \qquad \ldots (11)$$

Equation 11 was applied to the various KEWB cores; the results are given in Table I. The small difference between computed and observed values are well within experimental error. For convenience, G_{H_2} values as a function of uranium concentration are reproduced in Figure 4.[7] Values of Henry's constant for various uranyl salt solutions are reproduced in Figure 5.[8]

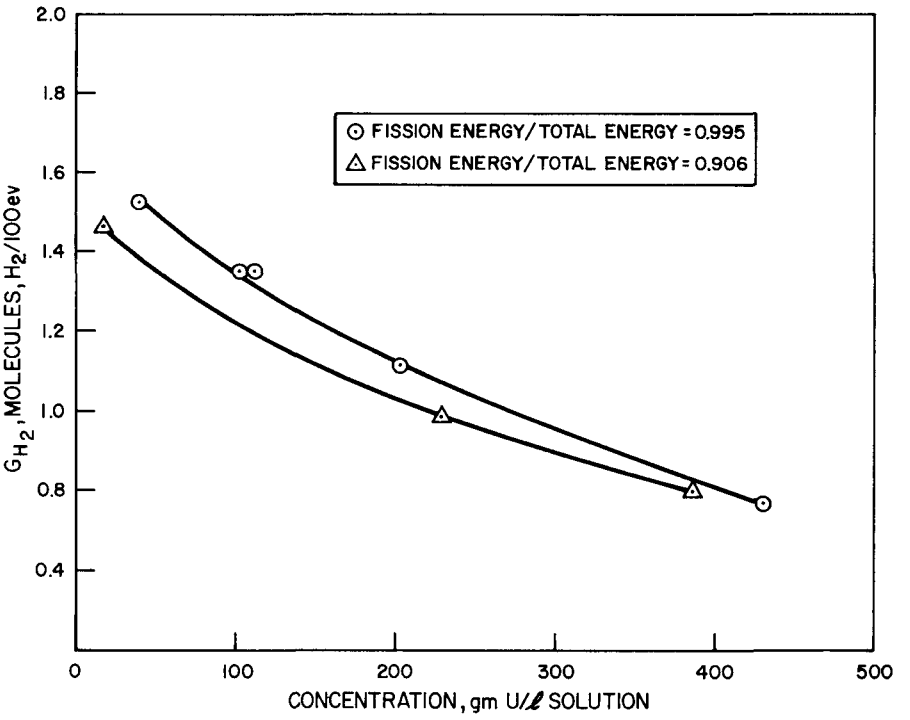

Figure 4. Effect of Uranium Concentration on Hydrogen Gas Yields From Irradiated Uranyl Sulfate Solutions

TABLE I

COMPARISON OF PREDICTED AND OBSERVED ENERGY RELEASE NECESSARY FOR VOID FORMATION IN KEWB REACTORS

Core	Fuel Solution Mass (gm)	$\frac{\phi_p}{\bar{\phi}}$	C_c gm H_2/100 gm Solution T_ℓ = 30°C, p_ℓ = 1 atm	E_c Predicted (Mw-sec)	E_c Observed (Mw-sec)
"A" Underfull	13,000	2.0	0.0020	0.6	0.6
"B" 18 Liter	20,000	2.5	0.0024	0.8	0.9
"B" 26 Liter	27,000	2.5	0.0026	1.1	1.2
"B" Bare	29,000	3.0	0.0018	0.9	1.0

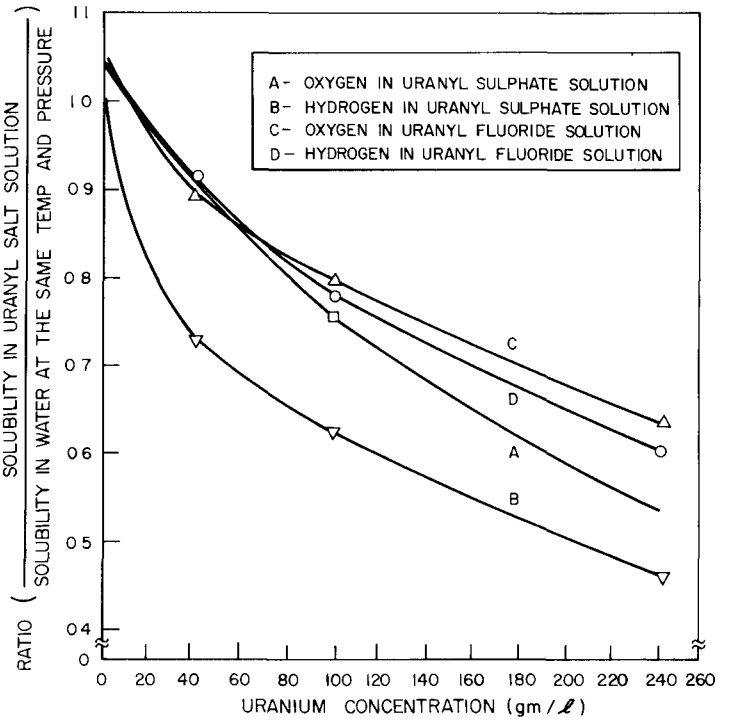

Figure 5. Ratio of Solubility of Hydrogen in Uranyl Salt Solutions to its Solubility in Water as a Function of the Uranium Concentration

III. CALCULATION OF VOID COMPENSATED REACTIVITY FROM A KNOWLEDGE OF THE INERTIAL PRESSURE

The sudden introduction of gas bubbles into the reactor core and their subsequent growth leads to the creation of a pressure field which forces an increase of solution volume. The rate of this void growth can be calculated from the pressure data. Consider a system obeying the hydrodynamic equation

$$\delta \frac{d\bar{v}}{dt} = -\nabla p \qquad \ldots (12)$$

where

δ = density of the medium,

$\bar{v}$ = velocity of a volume element at position r and time t, and

p = absolute pressure at position r and time t.

In the KEWB "B" cores, changes in the solution density are known to be small (< 10%) during a reactor transient, and motion is restricted to the vertical, or z direction, only. Therefore, $\bar{v}$ may be replaced by dz/dt and the assumption made that δ is a constant. It can be further assumed that p is separable in time and space; i.e., $p = p(z)f(t)$. This assumption is supported by the fact that three pressure transducers located at various places on the periphery of the core during a short period transient show similar pressure pulses; i.e., no time displacement of the pulses could be observed, although the amplitudes differed. Equation 12 becomes

$$\frac{d^2z}{dt^2} = -\frac{1}{\delta}\frac{dp(z)}{dz} f(t) \qquad \ldots (13)$$

A reasonable choice for $dp(z)/dt$ is $-(p_o/h)$, where p_o is the magnitude of the pressure change seen by the pressure transducer located at the bottom of the core, and h is the height of the fuel solution. This choice (which implies that p is of the form $p = -p_o(z/h) + p_o + p_{ex}$, the plane $z = 0$ corresponding to the bottom surface of the core, and p_{ex} being the external pressure) is in agreement with the observation that the magnitude of the pressure decreases in the direction of the free surface. The solution of Equation 13 is then

$$z(t) = \frac{1}{\delta}\frac{p_o}{h}\int_o^t (t - t')f(t')dt' \ . \qquad \ldots (14)$$

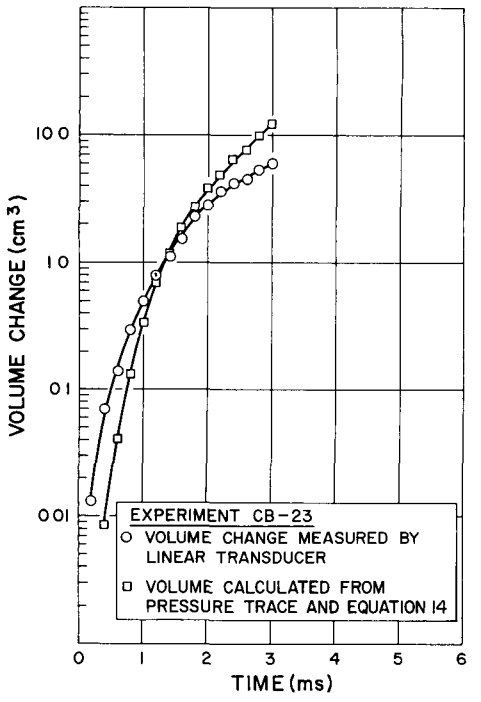

Figure 6. Comparison of Measured and Calculated Volume Change in Bellows Capsule

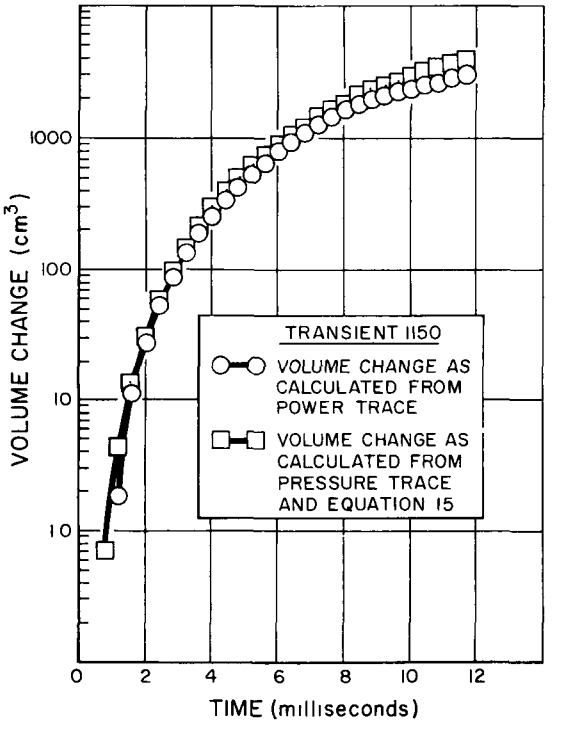

Figure 7. Volume Change in Core as Calculated From Pressure Trace and Power Trace

In the case of the capsule experiments, a direct measurement of the capsule volume change permitted verification of Equation 14; i.e., the z derived from the pressure traces and Equation 14 agreed with the measured volume change as shown in Figure 6. (The small discrepancy at large volume is due to the spring in the capsule.) In the KEWB, however, the volume change was not directly observed; it must be inferred from the void compensated reactivity. The void compensated reactivity, r_v, is proportional to to the overall volume change, or the displacement z times the cross section area A of the core.

$$r_v = \frac{c}{\delta}\frac{A}{h}p_o\int_o^t (t - t')f(t')dt' \quad \ldots (15)$$

where c is the constant used in converting from void volume to reactivity units; this was determined both experimentally and theoretically, and the two values were in reasonable agreement. Moreover, the linear relationship of r_v and z was verified over the range of interest.

The void compensated reactivity obtained from Equation 15 using pressure data from a representative reactor transient is shown in Figure 7. This graph also shows the void compensated reactivity for the same run computed from the power trace and the inhour equation as discussed in detail in Reference 3. The agreement of the two curves over three orders of magnitude substantiates the soundness both of the directly

observed quantities, power and pressure, and of the mathematical analysis required to convert these quantities to reactivity.

Thus a knowledge of the pressure field, core dimension, and coefficient of void compensated reactivity permits a calculation of the void compensated reactivity as a function of time. The computation of the pressure field is discussed in the next section; the core dimensions are, of course, known for any particular core. The coefficient of void compensated reactivity is available from experimental measurements.

IV. THE INERTIAL PRESSURE FIELD

The nucleation and subsequent growth of bubbles gives rise to the so-called inertial pressure field.

A rigorous mathematical formulation of this problem must consider diffusion growth together with interaction of the bubbles, creation of gas, coupling of bubble wall to fluid, and distribution in time and space of nucleation. The consideration of all these parameters makes the rigorous solution of the problem enormously complex. Fortunately, a rather simple model allows a very close estimate of the peak inertial pressure in terms of reactor power density at the start of nucleation. The time at which nucleation occurs can be calculated from the conditions necessary for bubble nucleation as has been shown in Section II of this report. The general shape of the pressure can also be estimated from a simple model to an accuracy sufficient for calculating the dynamic void characteristics.

In this simple model it will be assumed that all bubbles are nucleated in 2×10^{-4} sec, starting when the energy release E reaches E_c, the energy release at which nucleation occurs. The rapid depletion of gas by diffusion into the bubbles and the pressure increase due to nucleation and growth of the bubbles results in cessation of further nucleation of bubbles thereafter. In the time interval of 2×10^{-4} sec, the calculation based on diffusion theory and the amount of gas in solution indicates that a bubble of initial volume 5×10^{-16} cm^3 will grow to $\sim 10^{-14}$ cm^3. The total volume of gas bubbles will thus be

$$v_g = P_o \lambda v_b' \qquad \ldots (16)$$

where

P_o = fission rate at the time E reaches E_c,

$\lambda = 2 \times 10^{-4}$ sec, and

v_b' = effective bubble volume, 10^{-14} cm^3.

The gas volume v_g is created so rapidly that the core volume is essentially unchanged during the time of creation. The corresponding pressure change in the liquid is

$$p_m = \frac{1}{K_s}\frac{v_g}{V_{core}} = \left(\frac{v_b'\lambda}{K_s}\right)\left(\frac{P_o}{V_{core}}\right) = C'\left(\frac{P_o}{V_{core}}\right), \qquad \ldots(17)$$

or the inertial pressure is a linear function of the power density at the start of nucleation.

One might expect the cutoff time, λ, and the volume, v_b', to be weakly dependent on the power density, since a larger number of bubbles produced at higher values of P_o will exhaust the medium more rapidly than a smaller number. However, this is compensated for by the larger gas production at higher values of P_o and in the time interval past E_c. Also, as will be shown, the compressibility K_s increases as the bubble volume gets larger, so that the ratio v_b'/K_s varies much more slowly than v_b'.

Moreover, this increase in K_s also contributes to an effective cutoff time; bubbles nucleated a few tenths of a millisecond after E_c will grow in a medium whose compressibility has increased so that these later bubbles will contribute less pressure per unit volume than the earlier ones. For these reasons, the assumption that v_b', λ, and K_s are constant does not lead to serious errors. In Figure 8, the solid line shows the growth of a bubble at 1-atm liquid pressure at fixed gas concentration corresponding to E_c. The arrow indicates the assumption of the simple model. Slowing of growth is due to depletion of gas and onset of inertial pressure. A linear relation between power density and peak inertial pressure has been observed experimentally, as is shown in Figures 9 through 12. The four sets of data presented in these figures, while showing a linear dependence of pressure and power density, do not lead to identical estimates of the constant C' in Equation 17. The four sets of data are essentially superimposable if Equation 17 is corrected for the variation in G_{H_2} among the cores according to

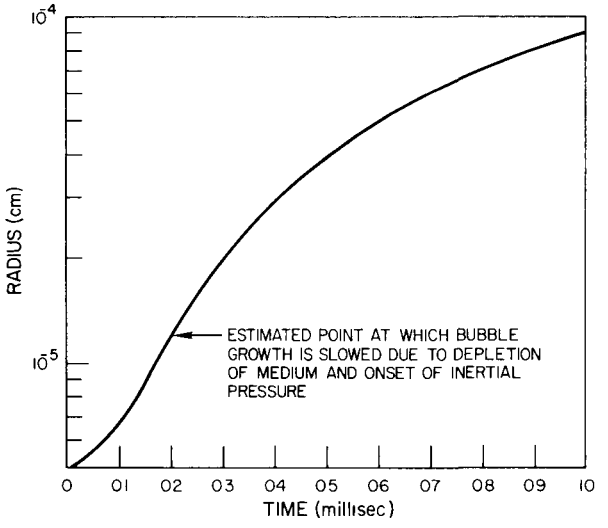

Figure 8. Bubble Growth Under Conditions Present at Nucleation

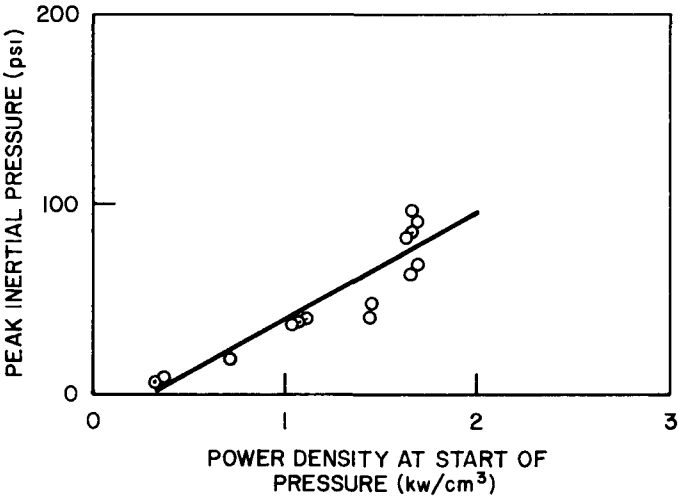

Figure 9. Peak Inertial Pressure vs Power Density at Start of Pressure for 11 Liter KEWB "A" Core

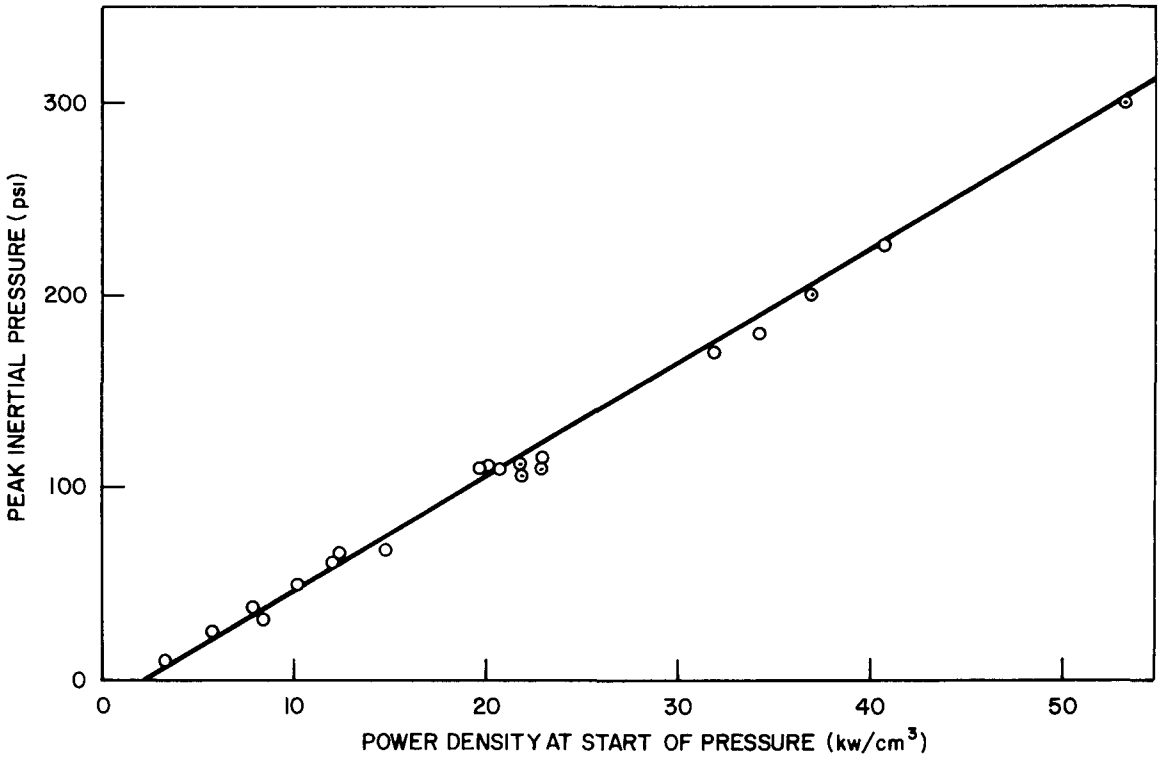

Figure 10 Peak Inertial Pressure vs Power Density at Start of Pressure for 18 Liter KEWB "B" Core

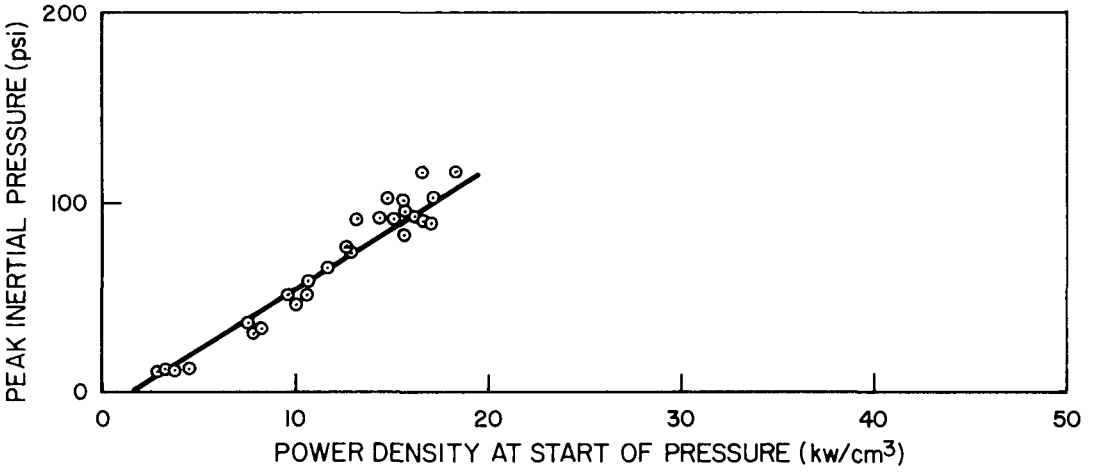

Figure 11. Peak Inertial Pressure vs Power Density at Start of Pressure for 26 Liter KEWB "B" Core

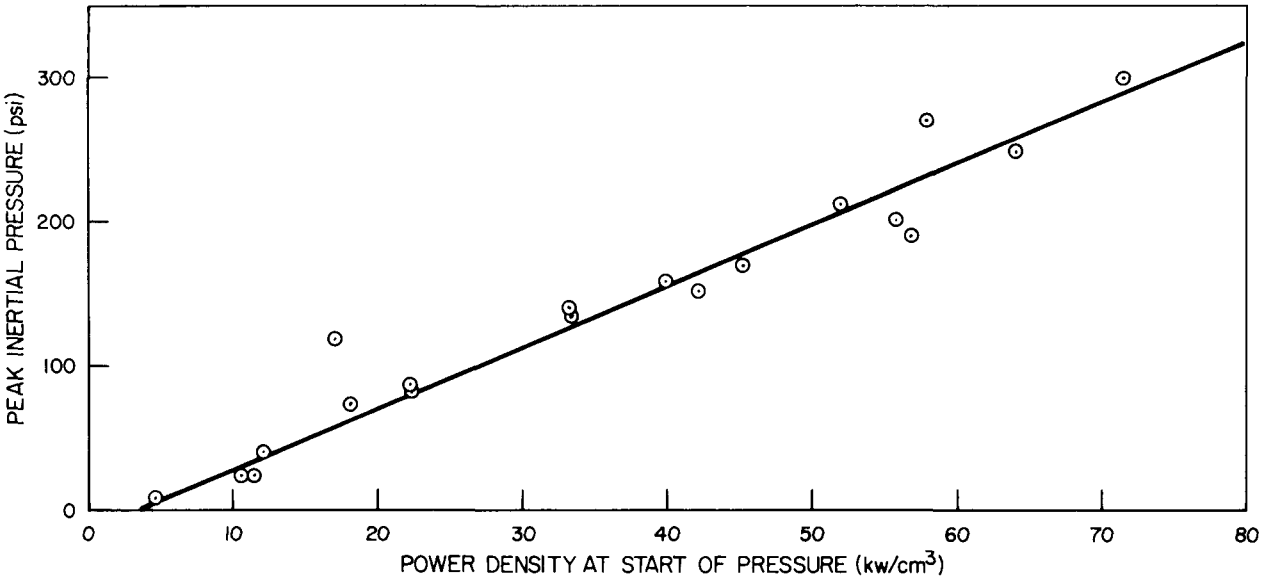

Figure 12. Peak Inertial Pressure vs Power Density at Start of Pressure for Bare KEWB "B" Core

$$p_m = C' \frac{G_{H_2}}{G_o}\left(\frac{P_o}{V_{core}}\right) - p_c \qquad \ldots (18)$$

where G_o = 1 mol of H_2/100 ev, and G_{H_2} is the appropriate value for the uranyl sulfate concentration in the core of interest. Figure 13 shows the data in Figures 9 through 12 replotted according to Equation 18. According to this figure, the best estimates for C' and p_c are 4.2 psi-cm^3/kw and 15 psi, respectively.

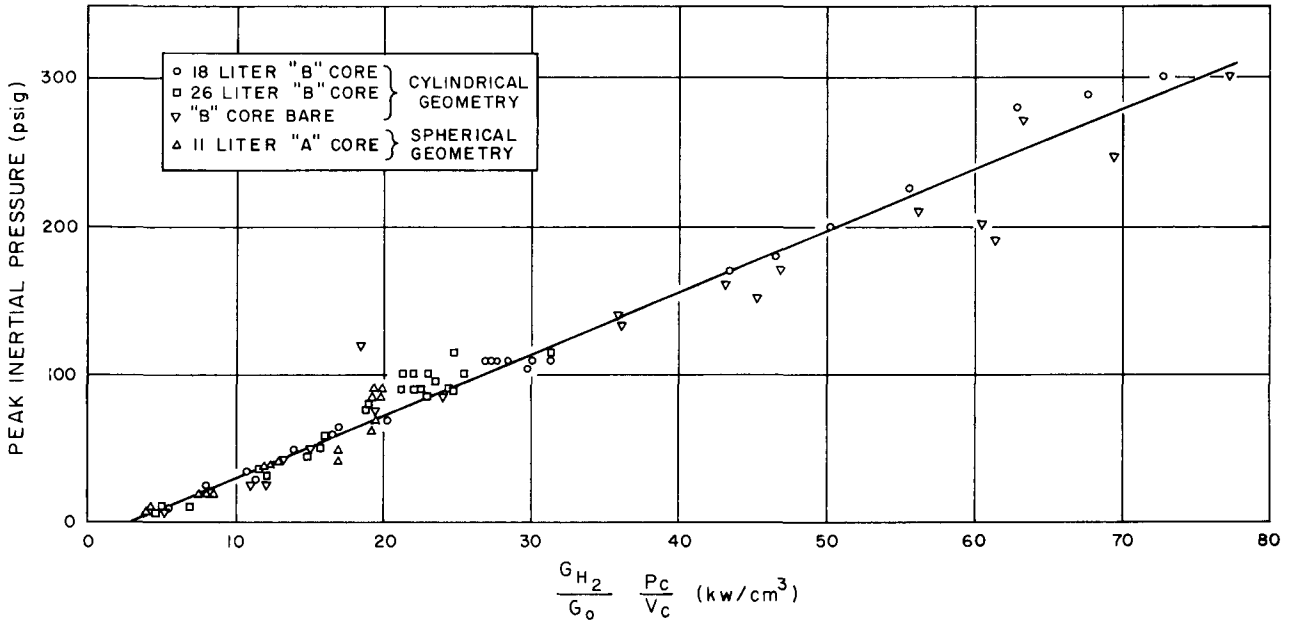

Figure 13. Plot of $G_{H_2}/G_o\ (P_o/V_{core})$ vs Peak Inertial Pressure

The constant C' can be calculated from the simple model. Using $v_b' = 10^{-14}$ cm^3, $\lambda = 2 \times 10^{-4}$ sec, and $K_s = 50 \times 10^{-6}$ atm^{-1}, it is seen, from Equation 17 that C' = 4×10^{-14} cm^3 sec/bubble. Now, 1 watt = 3×10^{10} fission/sec, and assuming one bubble per fission, C' = 20 psi-cm^3/kw is obtained in surprisingly fair agreement with C' = 4.2 psi-cm^3/kw estimated from the data. It should be noted that the compressibility of a bubble liquid mixture is strongly dependent on bubble size, void volume fraction, and liquid pressure; the exact expression is

$$K_m = K_\ell\,(1 - f) + \frac{f}{P_\ell + \frac{4}{3}\frac{\sigma}{R_g}} \qquad \ldots (19)$$

where

K_m = compressibility of liquid bubble mixture,

K_ℓ = compressibility of liquid,

P_ℓ = liquid pressure,

f = volume fraction of void,

σ = surface tension of liquid-gas interface, and

R_g = bubble radius.

Figure 14 shows the compressibility for a water gas mixture as a function of f. As can be seen, K_m increases rapidly for $f > 10^{-3}$. In the KEWB "B" core, this value of f would amount to a void volume of ~200 cm^3 which is never reached in 2 x 10^{-4} sec.

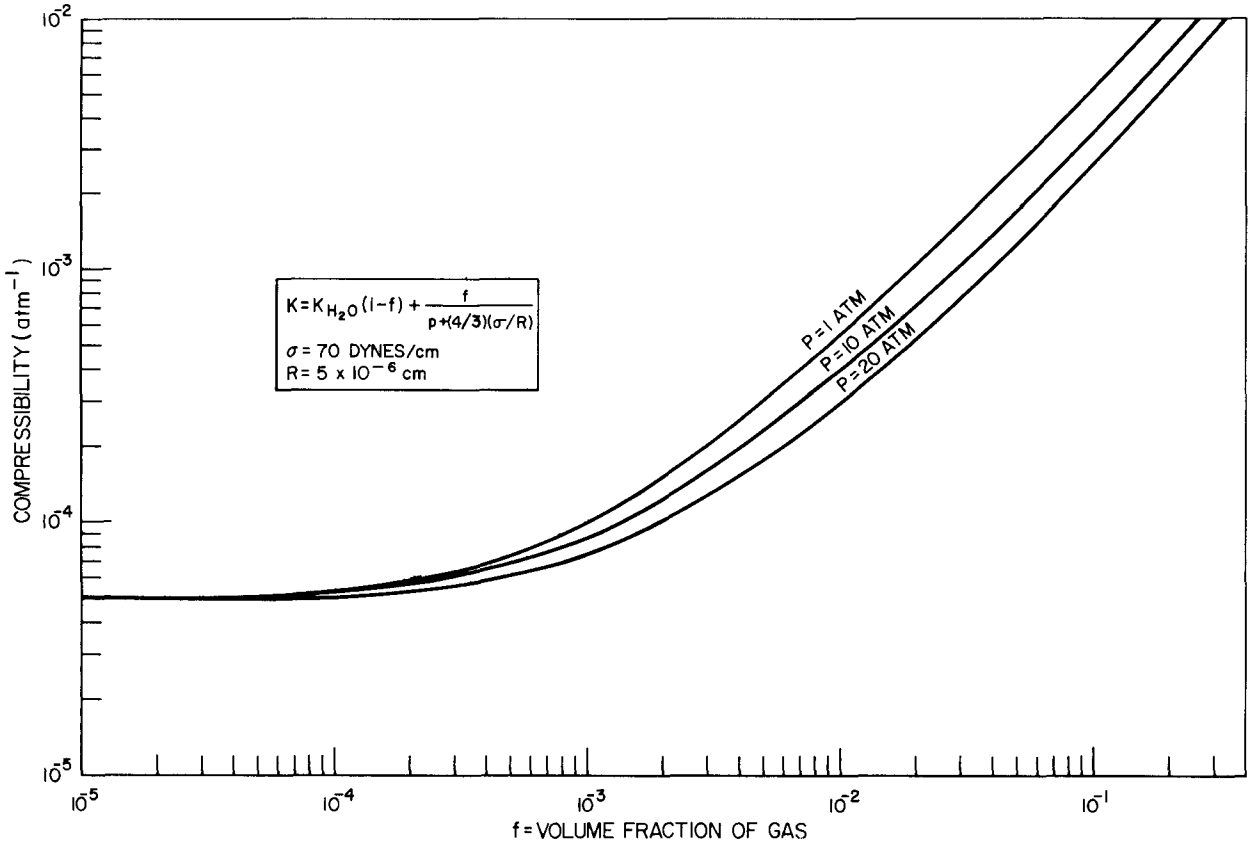

Figure 14. Compressibility of a Water-Bubble Mixture as a Function of the Volume Fraction of Gas

It can be seen, therefore, that the simple model yielding Equation 17 gives a correct dependence of the peak inertial pressure as a function of the power density at the start of void formation and leads to a fair estimate of the constant C'. Thus, the results of this simple model with correction for relative G value as expressed in Equation 18 is seen to provide an estimate of peak pressure over a considerable range of core types, volumes, and power level. These results suggest that an estimate of peak pressures for other reactor cores should not differ by more than 20% from the estimates of Equation 18 or Figure 13.

Since the width of the pressure pulse is determined by the inertia of the fluid, all practical reactor cores will exhibit pulse widths which are large compared to the swing time of the core vessel.[9] Therefore, the inertial pressure can be considered as a static pressure in estimating its destructive potential. For this purpose, a model, as outlined above, which permits a good estimate of the peak inertial pressure will suffice.

Calculation of the void compensated reactivity demands an estimate of the shape of the pressure pulse as well as of its peak value. The simplest description of the pulse shape is in terms of a rise time to peak and a decay time. The rise time is determined almost completely by the time required for the nucleation conditions (i.e., the critical gas concentration) to spread through the reactor core. In support of this interpretation of the rise time is the observation that in the capsule, which has an almost uniform flux through its volume, the rise time for the pressure is about 0.5 ms. The KEWB reactor was on a 3-ms period transient during this observation of the capsule, and the rise time of the pressure pulse in KEWB was 3 to 4 ms.

From the flux shape it is estimated that about one reactor period is required for this spread, and so an approximation is made of the rise of the pulse by the term $(1 - e^{\tau_1/t})$ where τ_1 is the transient period. Actual observed times from the start of pressure to peak are shown in Figures 15 and 16. The decay of the pressure is due to the expansion of the solution. Treatment of the fuel solution for times after peak pressure as if it were a homogeneous compressed mass leads to a single relaxation constant τ_2, given by

$$\tau_2 = \frac{v_g}{h} \qquad \ldots (20)$$

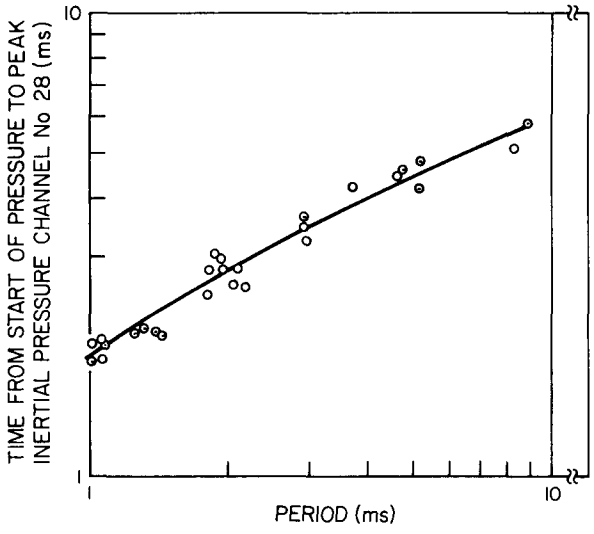

Figure 15. Time From Start of Pressure to Peak Pressure vs Transient Period for 18 Liter KEWB "B" Core

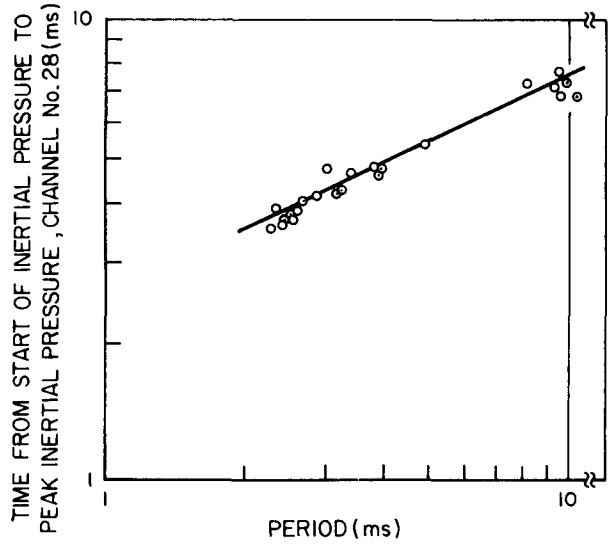

Figure 16. Time From Start of Pressure to Peak Pressure vs Transient Period for 26 Liter KEWB "B" Core

where

v_s = velocity of sound in the liquid bubble mixture, and

h = core height.

Observed values of τ_2 for the KEWB "B" cores are given in Table II.

TABLE II

OBSERVED PRESSURE DECAY CONSTANT FOR VARIOUS CORES

Core	τ_2 (ms)
18 ℓ reflected	4.0
26 ℓ reflected	4.7
Bare	2.0

The velocity of sound in a liquid gas mixture with 10% gas in volume is in the neighborhood of 100 m/sec. The core height is $\approx$ 30 cm; therefore, a theoretical value of τ_2 is 3 ms which has the proper order of magnitude. The argument leading to Equation 20 cannot, however, account for the observed factor of 2

between bare and reflected cores, although all three cores have almost the same height. However, by the time the decay of the pressure becomes significant, the core may be properly considered as a single compressed gas bubble. Such a system, which is considered in Appendix C, leads to an accurate description of the decay of the pressure pulse in all of the KEWB "B" cores.

A fair fit to the shape of the inertial pressure is given by

$$p_m = A_1 p_m \left[\left(1 - e^{-\frac{t}{\tau_1}} \right) \left(e^{-\frac{t}{\tau_2}} \right) \right] \qquad \ldots (21)$$

where P_m is the peak inertial pressure obtained from Equation 18, and A_1 is a constant normalizing the function in brackets to 1.0. Two examples are shown in Figures 17 and 18. The discrepancy between the observed and calculated peak pressure may be due in part to a signal induced by radiation in the instrumentation during the transient. In the spherical core, the free volume above the solution is usually filled rapidly; thereafter, the pressure is released by the ejection of fuel solution. Equation 21 should not be used to fit the data in the spherical core, or in other cases where motion of the liquid surface is restricted.

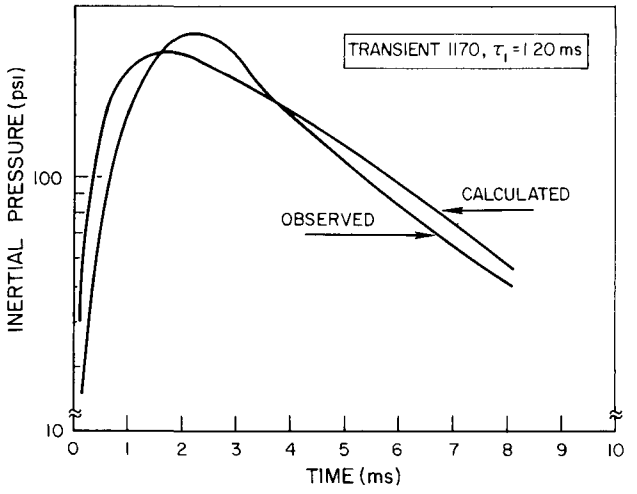

Figure 17. Comparison of the Inertial Pressure as Observed by a Pressure Transducer Located at the Bottom of the Core and as Calculated by Equation 21

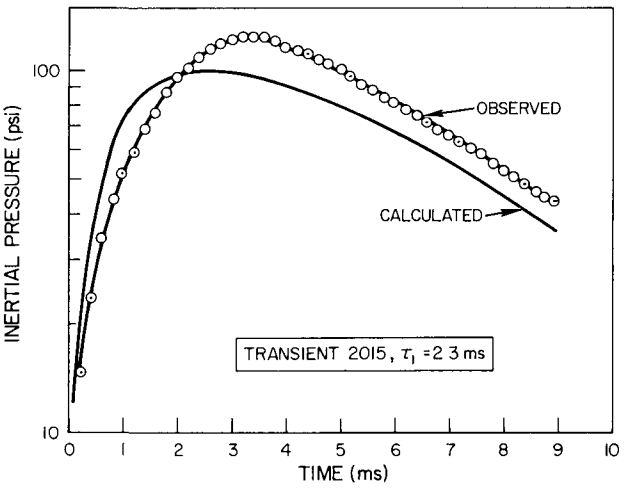

Figure 18. Comparison of the Inertial Pressure as Observed by a Pressure Transducer Located at the Bottom of the Core and as Calculated by Equation 21

APPENDIX A
INPILE CAPSULE EXPERIMENTS

1. DESCRIPTION OF CAPSULES

The experiments consist of measuring the pressure-volume-temperature characteristics of a small sample of fuel solution subjected to a radiation burst from the KEWB reactor. The fuel sample is contained in a capsule device which is located adjacent to the core vessel. Three types of capsules were used in performing the experiments. The first capsule type, called "Bellows Capsule" is shown in Figure 19. The test solution, ~30 cm^3, is contained in a very light

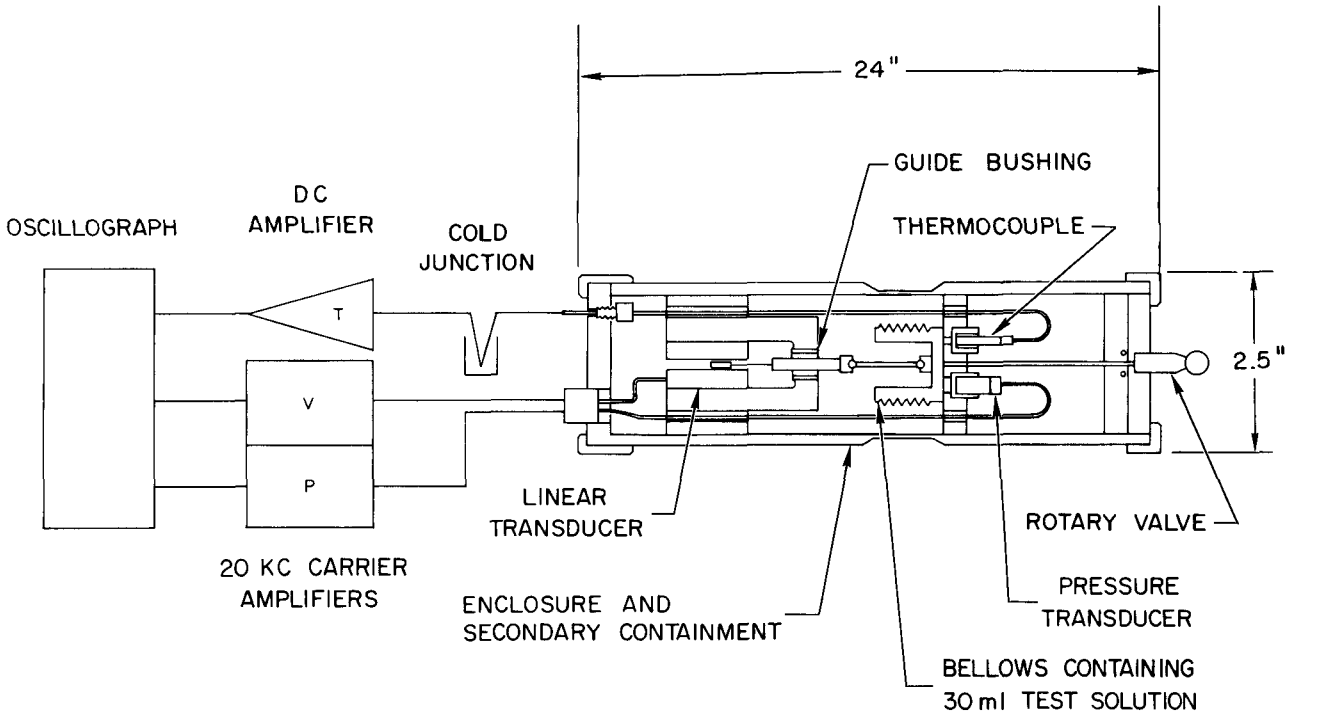

Figure 19. Bellows Capsule Schematic

bellows instrumented to provide the time function of the total volume change, fuel pressure, and fuel temperature. The bellows and the instruments are completely enclosed in a 2.5-in. diam cylindrical tube which provides secondary containment and also allows pressurization up to 10 atm. Filling and emptying of the capsule is achieved through a rotary valve located at one end of the secondary enclosure. Although this type of capsule performed very well, its major disadvantages were the low frequency response of the bellows, ~100 cps, and a

small volume expansion ratio. To overcome these difficulties, a second type of capsule called a "Bellofram Capsule" was constructed. This capsule was identical to the Bellows Capsule except that the bellows was replaced by a rolling diaphragm (Figure 20). The capsule contained ~8 cm^3 of fuel and afforded a high volume expansion ratio. Finally, to study the behavior of very small test solutions, a "Constant Volume Capsule" was constructed (Figure 21). The principle was to observe the pressure induced in a fixed volume, ~1.6 cm^3, containing a thin layer of test solution. Pressure was measured by two pressure transducers, one being in contact with the liquid.

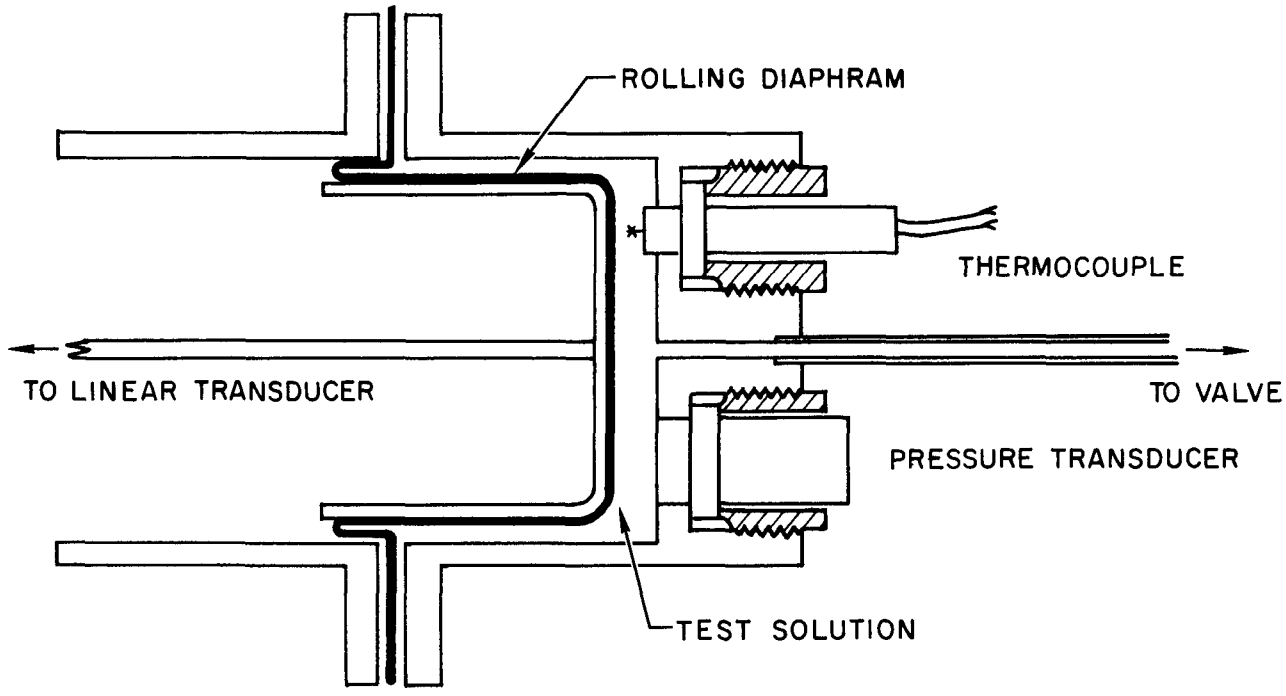

Figure 20. Bellofram Capsule

2. INSTRUMENTATION

Volume changes in the capsules were detected by the use of variable permeance linear motion transducers fabricated by Crescent Engineering. These are capable of measuring linear changes of 10^{-5} in. and are made of high-temperature, void-free inorganic materials.

Test solution pressures were detected by use of a flush diaphragm unbonded stain wire type differential pressure transducer fabricated by Statham Instrument Company. These sensors are capable of measuring differential pressures

in the range of 0 to 150 psid and were specifically fabricated of 347 stainless steel to insure compatibility with the acidified test solutions.

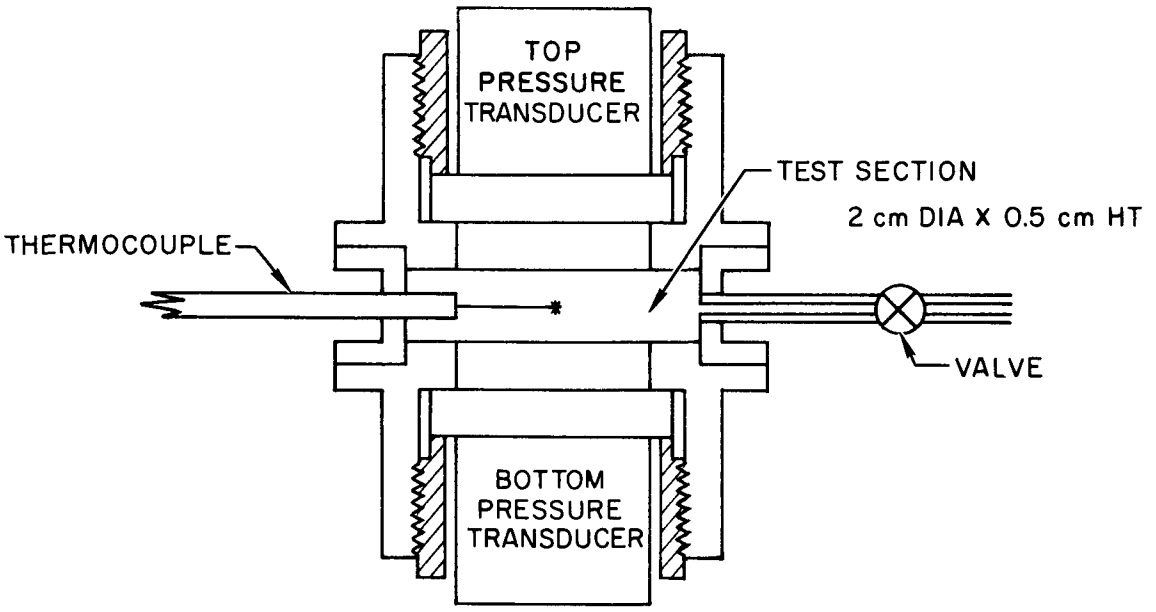

Figure 21. Constant Volume Capsule

Temperatures were detected by use of Pt-Pt, 10% Rh thermocouples which had a 1-mil exposed junction. This type is compatible with the acidified test solutions and exhibits a response time of 1 ms.

The linear motion and pressure transducers were used with 20-kc carrier amplifiers; the thermocouple signal was amplified by a dc amplifier. Data recording was achieved by use of a 14-channel light beam recording oscillograph. Typical data traces are shown in Figures 22 and 23.

3. EXPERIMENTAL PREPARATION AND IRRADIATION FACILITY

Each sample of test solution was irradiated only once. Capsule filling and flushing was accomplished by means of a solution transfer apparatus closed to the atmosphere (Figure 24) and contained in a dry box which affords a controlled environment for handling operations. The test solution was usually a solution of 93% enriched uranyl sulfate acidified with 0.5 molar H_2SO_4. It was first degassed by a freezing process and then introduced into the capsule under vacuum conditions.

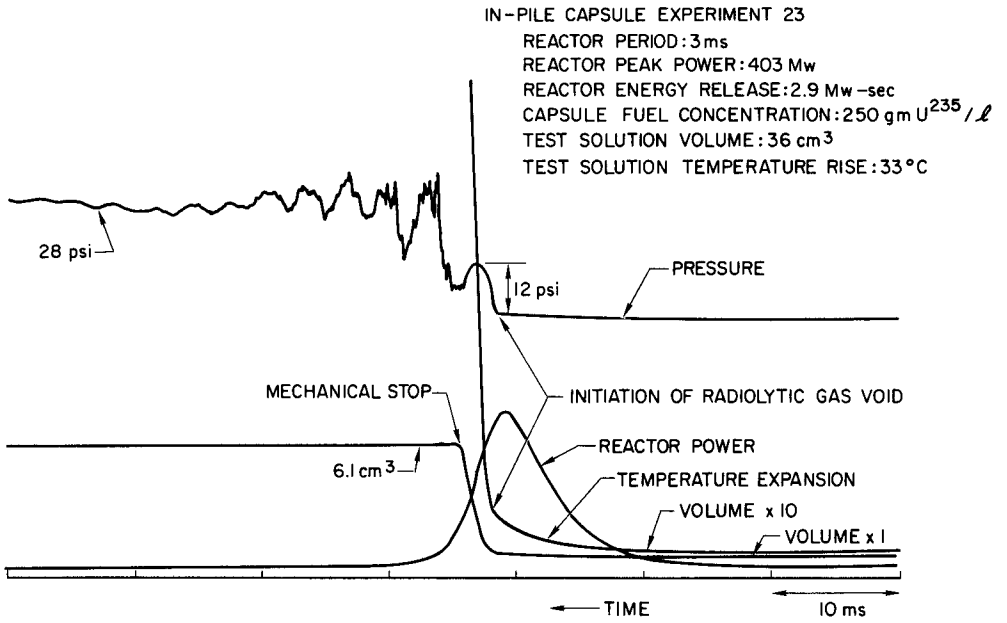

Figure 22. Representative Oscillograph Record for Bellows Capsule

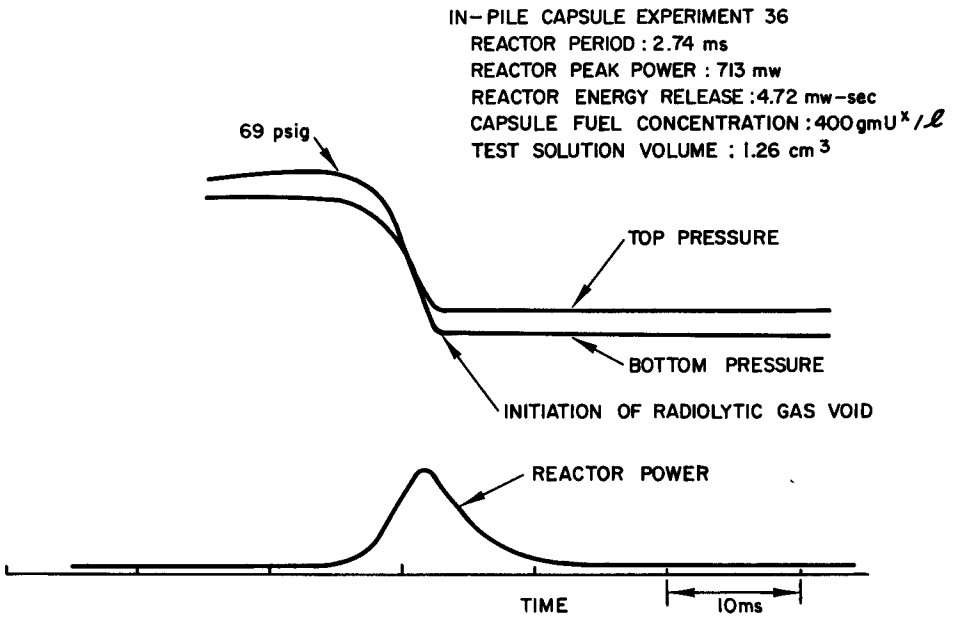

Figure 23. Representative Oscillograph Record for Constant Volume Capsule

The experiments were performed in the 4- by 4-in. horizontal exposure facility in the KEWB reactor. This facility is tangent to the reactor core and is an integral part of the reflector assembly. The capsule was placed so that the section containing the test solution was closest to the core. Gold wires were used to measure the integrated thermal flux experienced by the test solution during the transients. Typical integrated thermal fluxes were of the order of 3×10^{13} neutrons/cm^2.

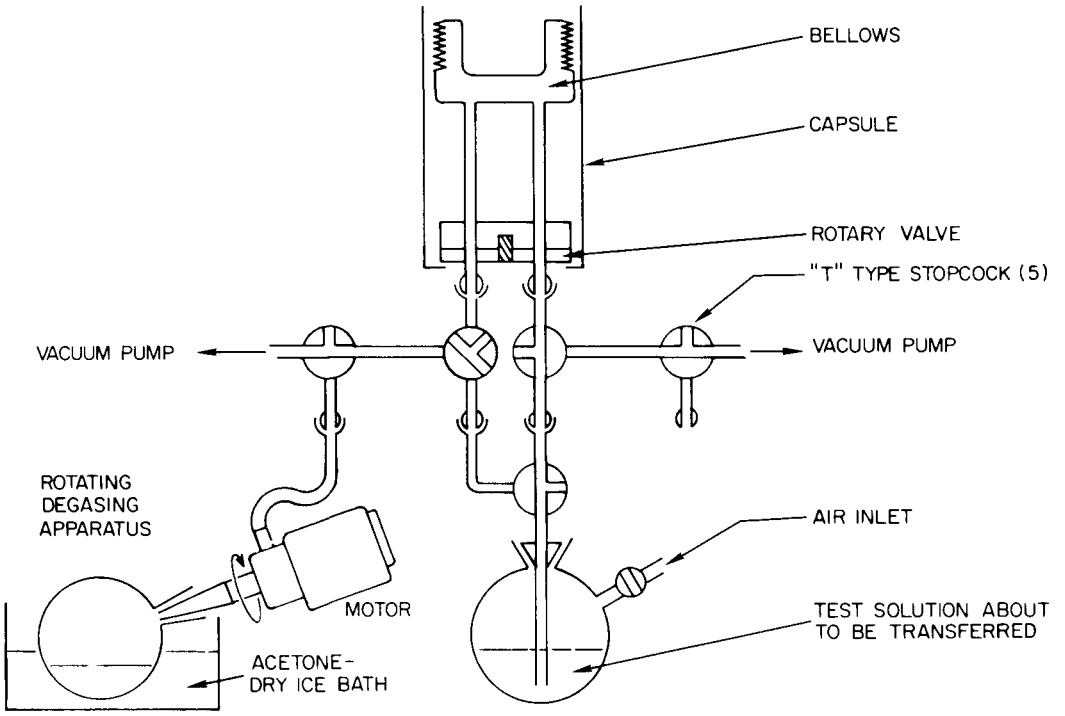

Figure 24. Schematic of Capsule Filling and Flushing System

APPENDIX B
SUMMARY OF KEWB REACTOR CHARACTERISTICS

Parameter	Spherical Core		Cylindrical Core		
	85% Full 11.45 Liters	100% Full 13.65 Liters	18 Liter Reflected	26 Liter Reflected	24 Liter Unreflected
Critical Mass (gm U^{235})	1680	1240	1450	1290	3900
Fuel Concentration (gm U^{235}/Liter)	166	106	94	57	203
H/U^{235} Ratio	152	263	272	465	124
Excess Reactivity ($)	3.50	3.75	5.80	4.50	3.75
Maximum Peak Reactor Power (Mw)	450	650	2500	1050	4000
Minimum Stable Reactor Period (ms)	2.0	2.0	0.90	2.1	0.57
Energy Released in a Maximum Burst (Mws)	3.5	5.7	9.0	6.1	7.0
Maximum Peak Pressure Observed (psi)	650	450	350	140	350
Maximum Vessel Acceleration Observed (g)	–*	–*	130	40	135
Mass Coefficient of Reactivity (gm U^{235})	0.014	0.016	0.016	0.024	0.0035
Water Coefficient of Reactivity (cc)	0.0027	0.0009	0.0006	-0.00035	0.001
Temp Coefficient of Reactivity 30°C (°C)	-0.020	-0.041	-0.041	-0.037	-0.053
Gas Production Coefficient (Liters H_2-O_2/kwh)	15.6	18.1	17.3	19.1	15.1

*Core Vessel not equipped with accelerometer

APPENDIX C
AN EQUILIBRIUM MODEL FOR INERTIAL PRESSURE

It may be assumed that each bubble is in equilibrium with the dissolved gas:

$$Kc = p_{in} + p_{\ell} + \frac{2\sigma}{R} = p_i \qquad \ldots(22)$$

where K is Henry's constant, c is the concentration of dissolved gas, p_{in} is the inertial pressure, p_{ℓ} the static, liquid pressure, and R_g the bubble radius. It may also be written for each bubble that

$$p_i v_b = n_g R_c T \qquad \ldots(23)$$

where v is the bubble volume, n_g the number of moles of gas in the bubble, R_c the gas constant, and T the absolute temperature.

According to the first assumption, all bubbles will be of uniform size and so Equation 23 can be replaced by

$$p_i v_b = N R_c T \qquad \ldots(24)$$

where N is the total moles of gas in bubbles, and V is the void volume. It has been seen previously that v_g can be obtained from p_{in} by

$$v_g = a_2 \int_o^t (t - t')\, p_{in}(t')dt' \qquad \ldots(25)$$

where a is a constant.

Furthermore,

$$N_g = G(E - E') \qquad \ldots(26)$$

where E is the energy release and G is the value of G_{H_2}. Thus, GE is the total gas production, and GE' represents the gas in solution by Equation 22.

Putting these together, the following can be written:

$$p_{in} = \frac{GRT}{v_g}\left[E - E_c\left(\frac{p_{in} + p_\ell + \frac{2\sigma}{R}}{p_\ell + \frac{2\sigma}{R_o}}\right)\right] - \frac{2\sigma}{R_g} - p_\ell \qquad \ldots(27)$$

with v_g given by Equation 25, and E_c the value of E at nucleation.

Equations 25 and 27 can be solved, but the resulting values of p_{in} near the start of pressure are much too high. This is because the bubbles are not nucleated simultaneously and, hence, the number of moles of gas in bubbles is much smaller than this model predicts. However, the model can be adjusted by taking explicit account of the spread of nucleation through the core. The spread takes about $1.5\tau_1$, when τ_1 is the reactor period. The core volume in which nucleation has occurred, therefore, is approximately proportional to $(t / 1.5\tau_1)^3$. Consideration of the various factors in Equation 27 leads to some simplifications, and so, finally the following is reached:

$$p_{in} \approx \begin{cases} \frac{GR_cT}{v_g}(E - E_c)\left(\frac{t}{1.5\tau_1}\right)^3 & \text{for } t \leq 1.5\tau_1 \\ \frac{GR_cT}{v_g}(E - E_c) & \text{for } t \geq 1.5\tau_1 \end{cases} \qquad \ldots(28)$$

where v_g is obtained from Equation 25.

Equations 25 and 28 were computed. Comparison of the computed values of p_i with observed values are shown in Figures 25 and 26. The interesting point is the rather good agreement of the slope of the computed pressure pulse for time past peak pressure with observations for all cores. Fundamentally, this agreement reflects the appropriateness of the basic equilibrium model for times after the peak pressure is reached.

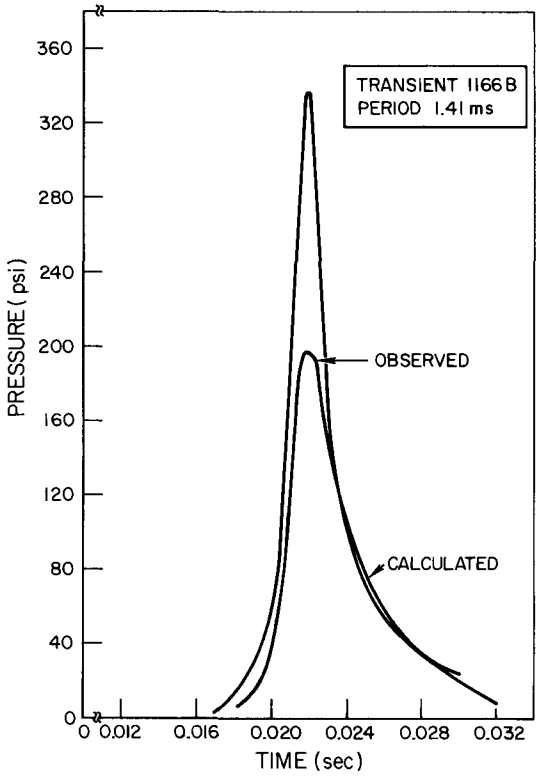

Figure 25. Comparison of the Inertial Pressure as Observed by a Pressure Transducer Located at the Bottom of the Core and as Calculated by Equation 28

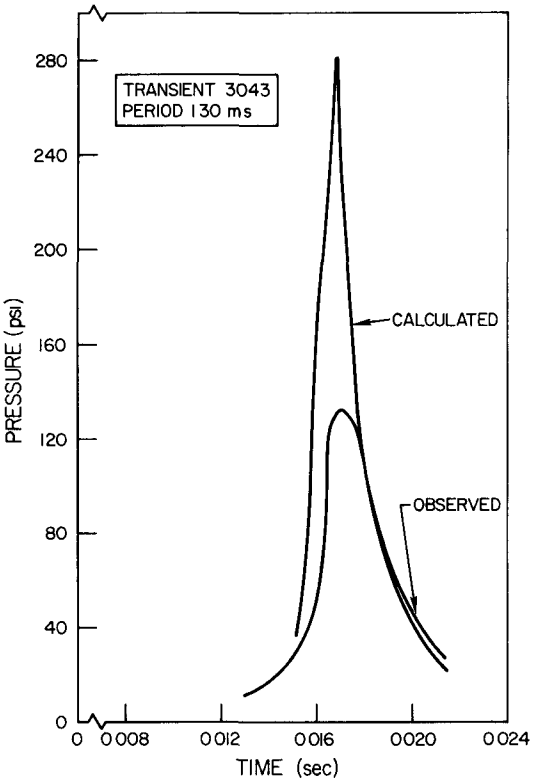

Figure 26. Comparison of the Inertial Pressure as Observed by a Pressure Transducer Located at the Bottom of the Core and as Calculated by Equation 28

NOMENCLATURE

A = Cross-sectional area of cone

a_1 = A conversion factor

a_2 = A conversion factor

C_c = Critical gas concentration in liquid necessary for gas bubble nucleation

$(C_v)_v$ = Specific heat of vapor at constant volume

c = Coefficient of void compensated reactivity

C' = A constant $\left(v_g' \lambda / K_s\right)$

D = Thermal diffusivity

E = Energy release in core

E_c = Energy release in core necessary for bubble nucleation

f = Volume fraction of gas in a liquid gas mixture

G = Same as G_{H_2} but in units of E

G_{H_2} = Number of hydrogen molecules formed per unit energy release

h = Height of core

K = Henry's constant

L = Latent heat of vaporization

ℓ = Lifetime of gas bubble

N = Instantaneous number of bubbles in core

N_g = Total moles of gas in all bubbles

n_g = Number of moles of gas in a bubble

P_o = Power at initiation of void formation

p_c = Constant

p_{ex} = Pressure above core solution

p_i = Internal gas pressure of gas bubble

p_{in} = Inertial pressure

p_ℓ = Liquid pressure

p_m = Peak inertial pressure

p_o = Magnitude of pressure change seen by a pressure transducer at bottom of core

$p_s(n,t)$ = Absolute pressure in core at position r and time t

p_s = Axial distribution of pressure in core

p_v = Vapor pressure

R_c = Universal gas constant

R_g = Gas bubble radius

R_v = Vapor bubble radius

$r_v(t)$ = Void compensation reactivity as a function of time

S = Number of bubbles born per unit time

T_ℓ = Liquid temperature

T_v = Vapor temperature

V_{core} = Core volume

v_b = Volume of gas bubble

v_b' = Effective volume of gas bubble

v_g = Gas volume in core, or void volume

v_s = Velocity of sound in medium

δ_ℓ = Liquid density

δ_s = Density of core solution

δ_v = Vapor density

E = Energy release per fission

$\Phi(r,t)$ = Neutron Flux distribution in space and time

$\phi(r)$ = Neutron flux distribution in space

$\phi_p/\bar{\phi}$ = Peak to average neutron flux ratio

K_ℓ = Compressibility of liquid

K_m = Compressibility of a liquid gas bubble mixture

K_s = Compressibility of core solution

λ = A time interval, 2×10^4 sec

σ = Surface tension

Σ_f = Fission cross section

τ = Vapor bubble lifetime

τ_1 = Transient Period

τ_2 = Core relaxation constant

REFERENCES

1. B. Hahn, "Gas Bubble Chamber Research," Final Technical Report, Contract AF61(514)-1262

2. J. W. Flora (ed.), "Kinetic Experiments on Water Boiler - 'A' Core Report - Part 1 - Program History, Facility Description and Experimental Results," NAA-SR-5414 (in press)

3. M. Dunenfeld and R. K. Stitt, "Summary Review of the Kinetic Experiments on Water Boiler," NAA-SR-7087 (in press)

4. P. S. Epstein and M. S. Plesset, "On the Stability of Gas Bubbles in Liquid-Gas Solutions," J. Chem. Phys., 18 (1950), p 1505-09

5. J. Ghormley, "Nucleation of Bubbles in Superheated Aqueous Solutions by Fast Particles," J. Nuclear Energy, 6 (1958), p 300-302

6. S. A. Zwick and M. S. Plesset, "On the Dynamic of Small Vapor Bubbles in Liquids," J. Math. and Phys., 33 (1954), p 308

7. J. F. Hogerton and R. C. Grass (ed.), "Engineering," the Reactor Handbook, 1st Ed., Report AECD 3646 (Washington, D.C., Government Printing Office, 1955) pp 560-574

8. E. F. Stephan et al, "The Solubility of Gases in Water and in Aqueous Uranyl Salt Solutions at Elevated Temperatures and Pressures," Batelle Memorial Institute Report BMI 1067 (1956), p 54

9. M. A. Greenfield, "Kinetic Experiments on Water Boilers - 'A' Core Report - Part IV - Containment Aspects of Pressure Waves," NAA-SR-5419 (December 1960)